Electronic Supplementary Material (ESI) for Journal of Materials Chemistry C.

Supplementary information for theoretical prediction of two-element two-dimensional layered structures and efficient doping engineering on carbon phosphide

Sheng Liu [a], Bin Liu [a], Tongtong Wang [a], Sicong Zhu [a, b *], Yu Li [a, *]

a Hubei Province Key Laboratory of Systems Science in Metallurgical Process, The State Key Laboratory for Refractories and Metallurgy, Collaborative Innovation Center for Advanced Steels, International Research Institute for Steel Technology, Wuhan University of Science and Technology, Wuhan 430081, China

b Department of Mechanical Engineering, National University of Singapore, 117575, Singapore

E-mail address: sczhu@wust.edu.cn, liyu@wust.edu.cn

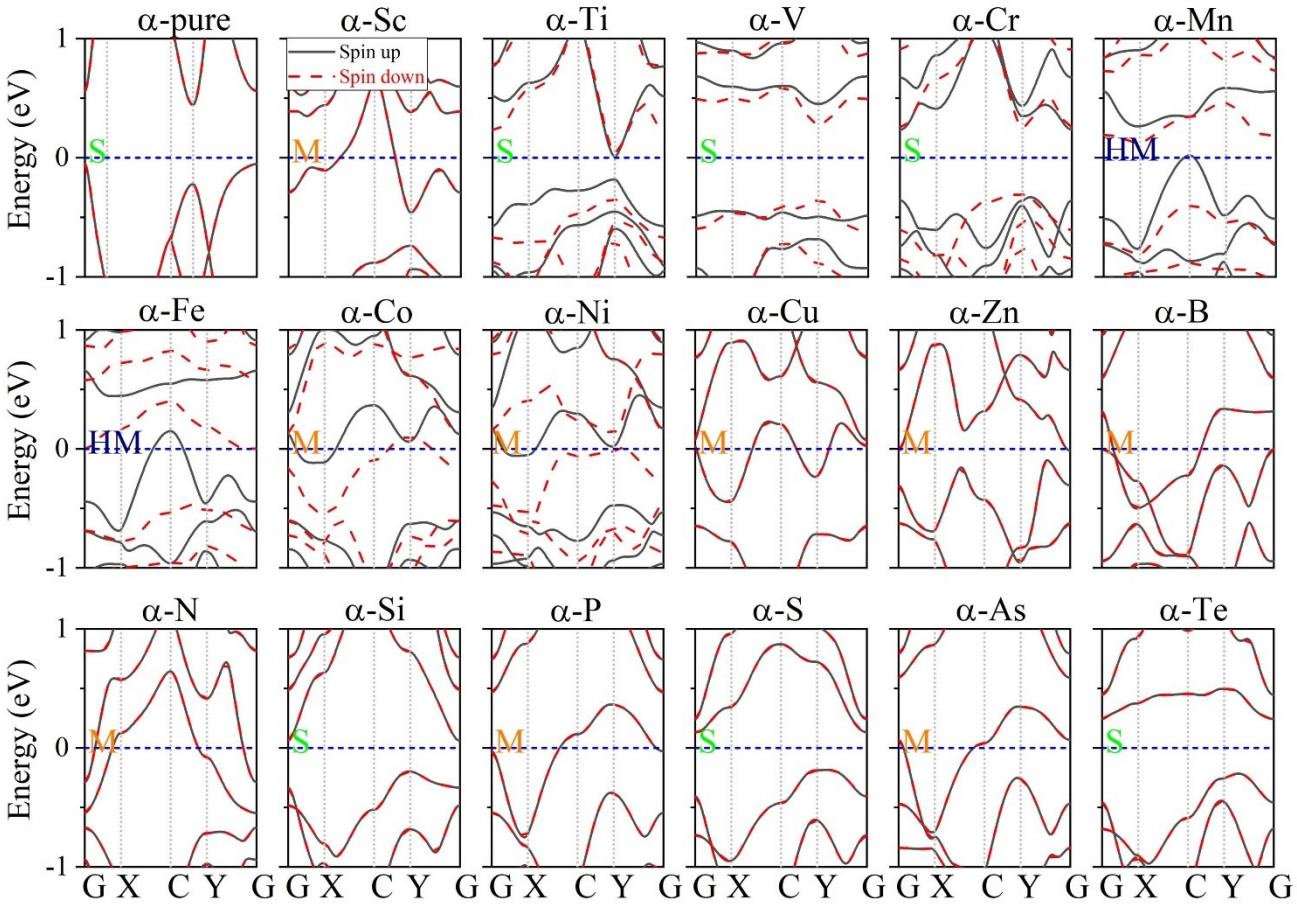

Fig. S1 The band structures of pure α-CP and C-atom substituted systems based on α-CP. The letters S, HM, and M represent the doping systems that have semiconductor, half-metal, or metal properties, respectively.

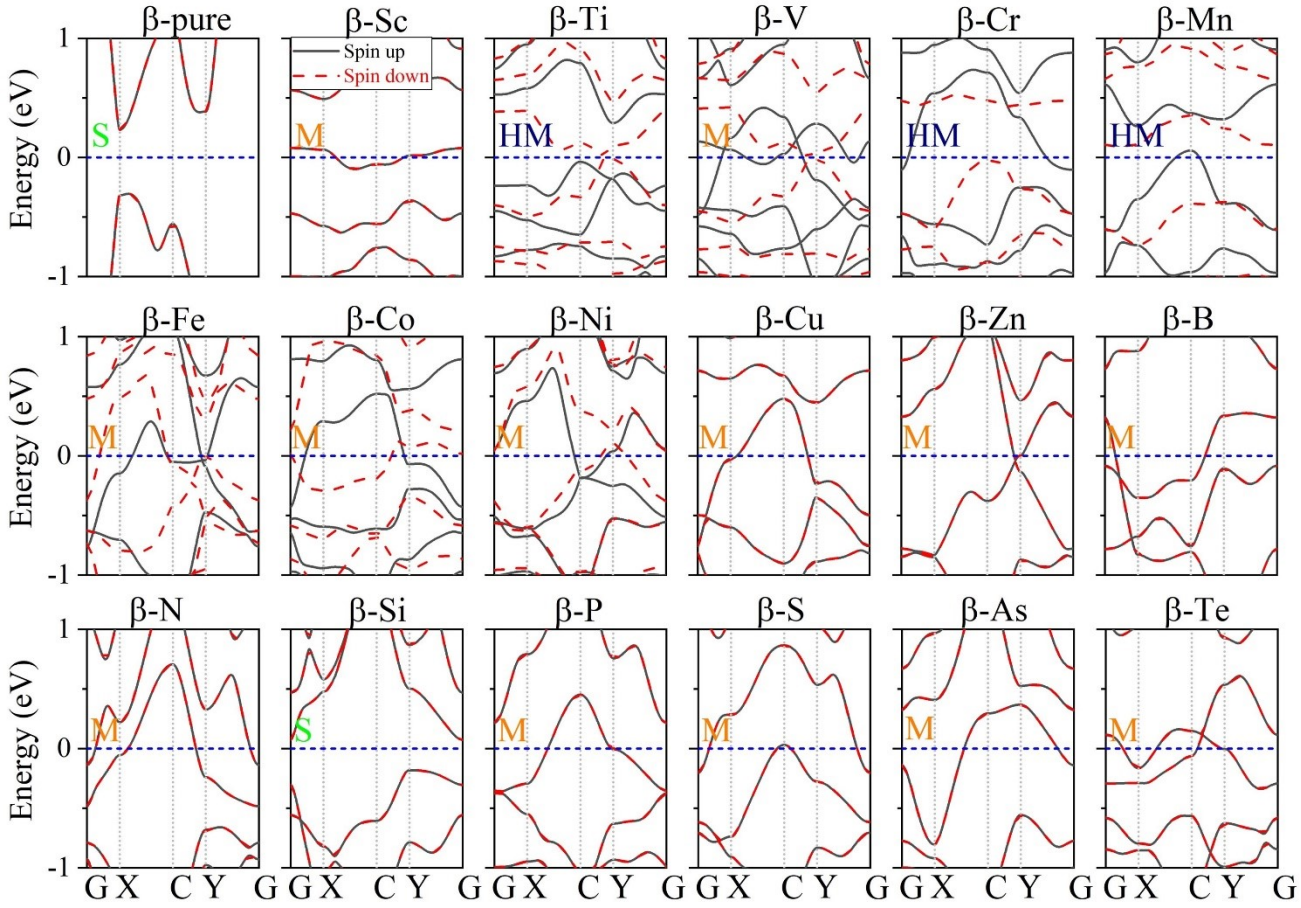

Fig. S2 The band structures of pure β-CP and C-atom substituted systems based on β-CP.

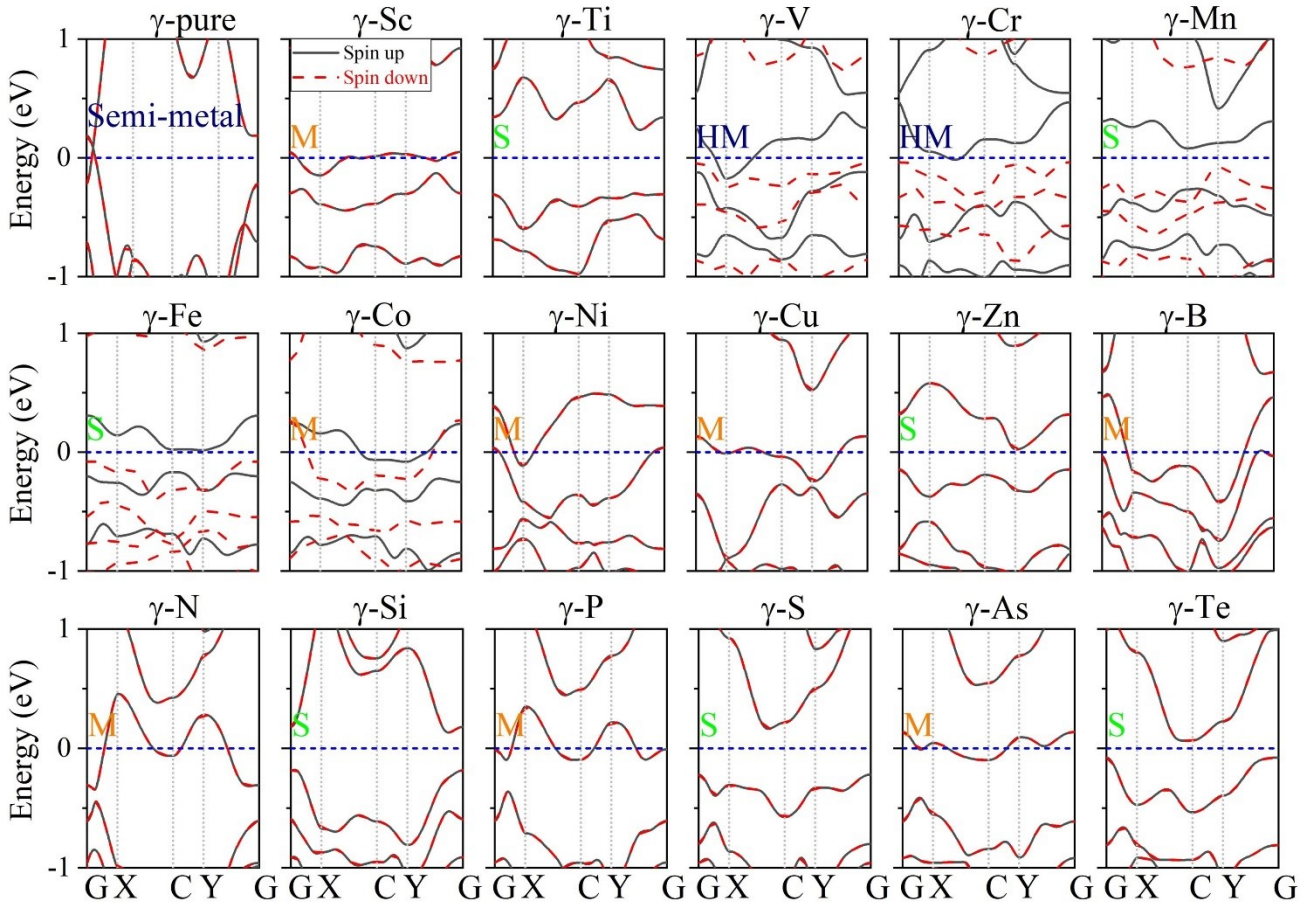

Fig. S3 The band structures of pure γ-CP and C-atom substituted systems based on γ-CP.

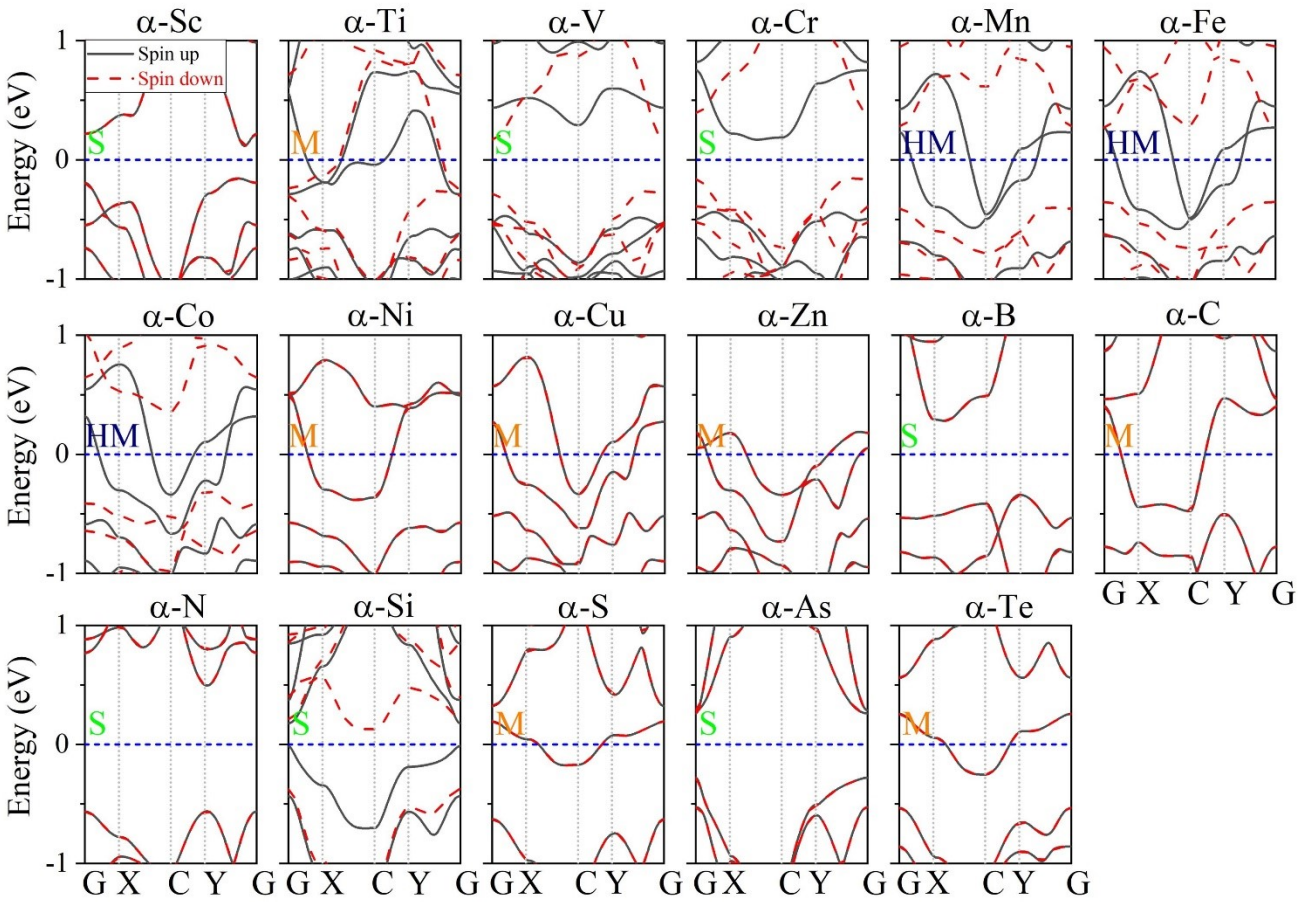

Fig. S4 The band structures of P-atom substituted systems based on α-CP.

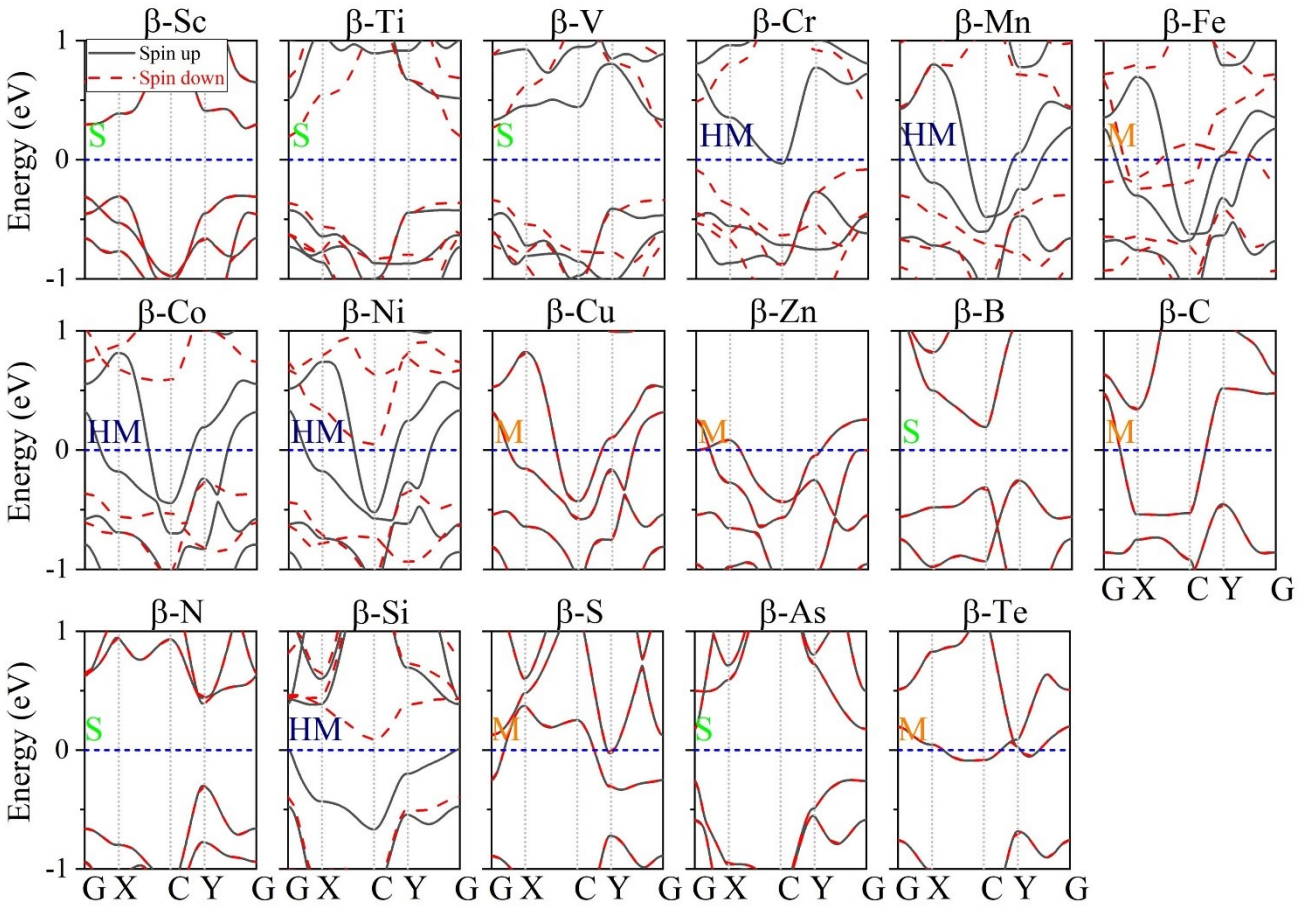

Fig. S5 The band structures of P-atom substituted systems based on β-CP.

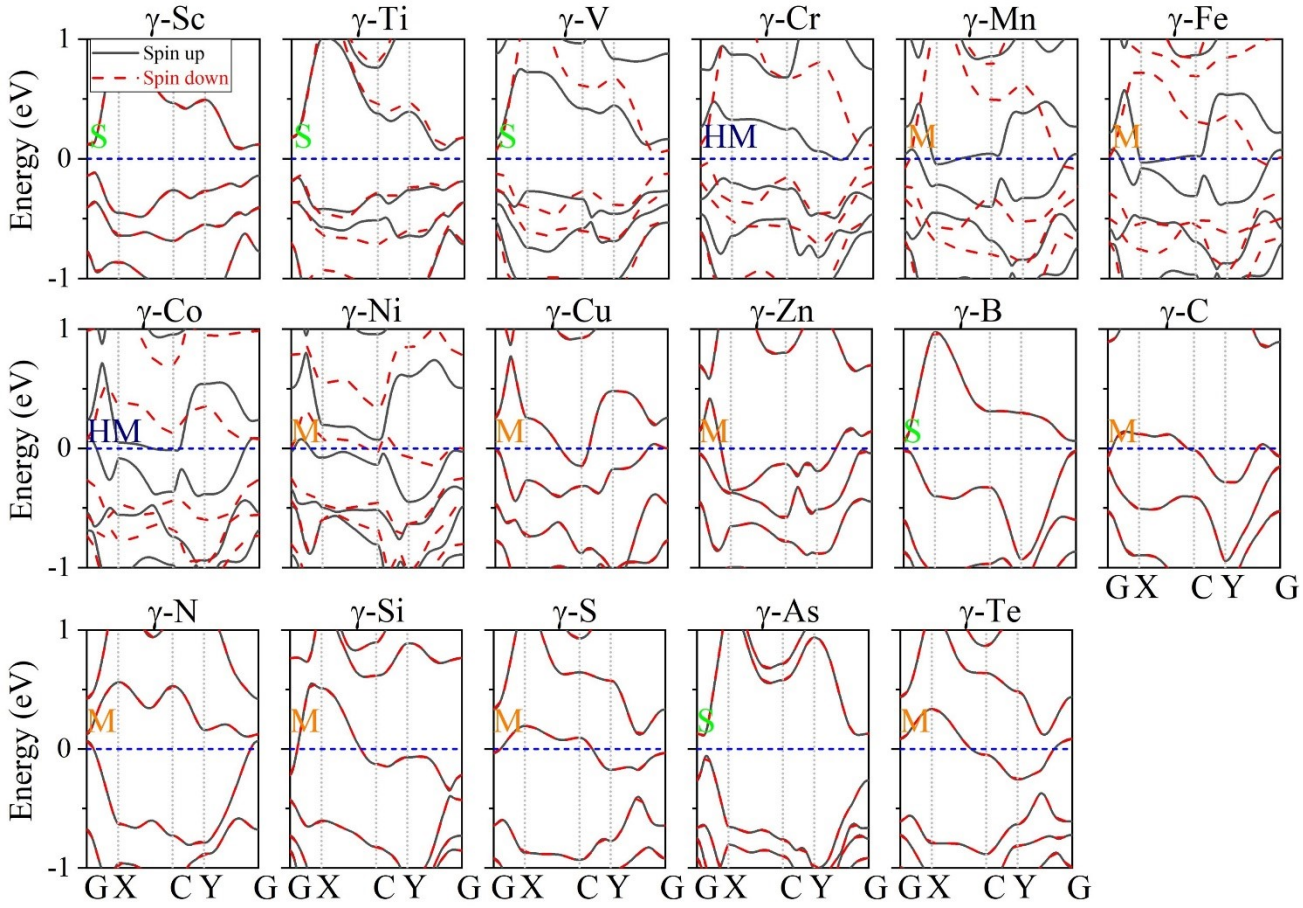

Fig. S6 The band structures of P-atom substituted systems based on γ-CP.

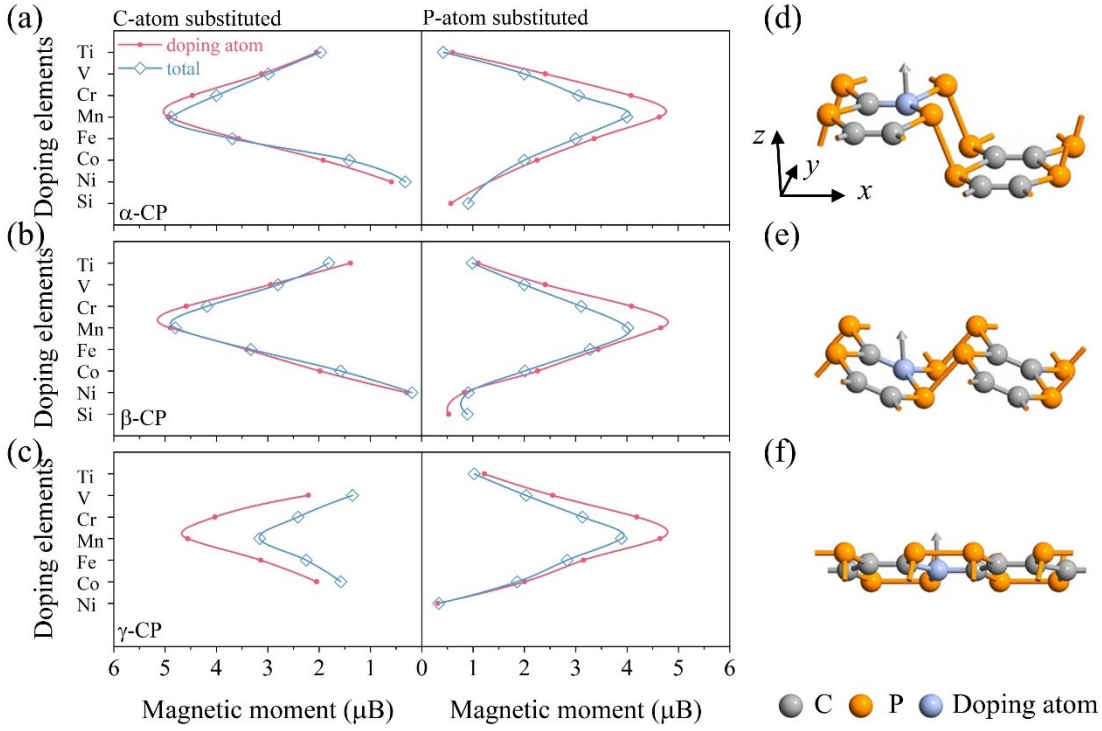

Fig. S7 The magnetic moment contributed by the doping atoms and the total magnetic moment of the doping system while in (a) α-CP, (b) β-CP, and (c) γ-CP doping. The C-atom substituted systems in the left panel and

the P-atom substituted systems in the right panel. Schematic of magnetic moment distribution of the doping systems while in (d) α-CP, (e) β-CP, and (f) γ-CP doping. Here are the examples of the C-substituted systems.

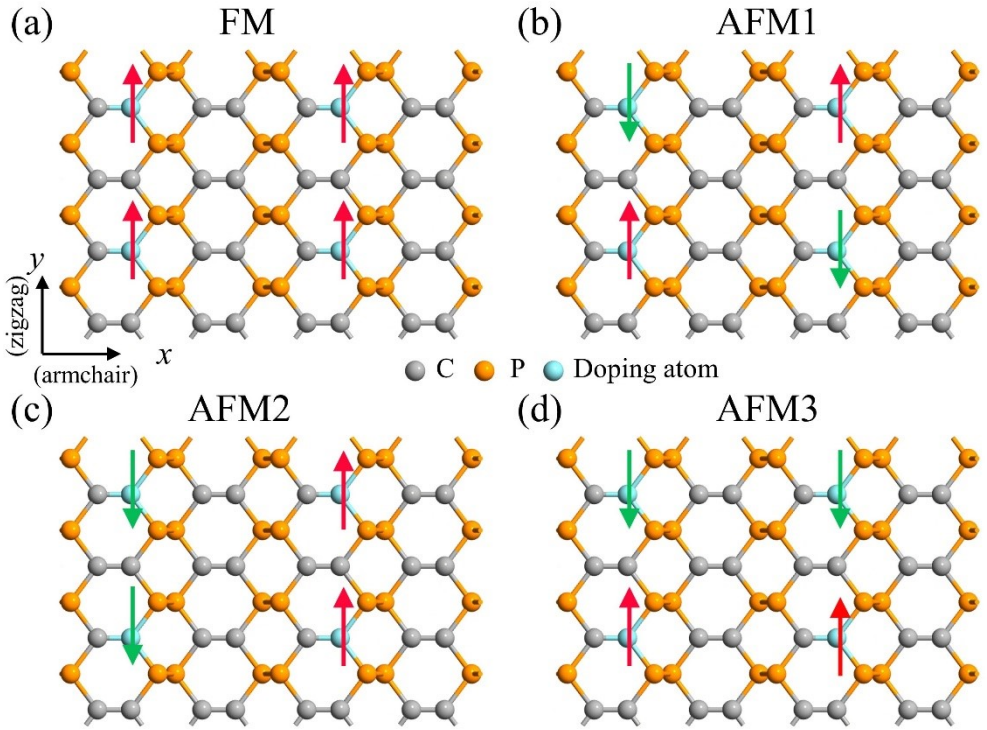

Fig. S8 The supercell with (a) FM, (b) AFM1, (c) AFM2, and (d) AFM3 order, respectively. The red arrow indicates the spin direction upward, the green arrow indicates the spin direction downward.

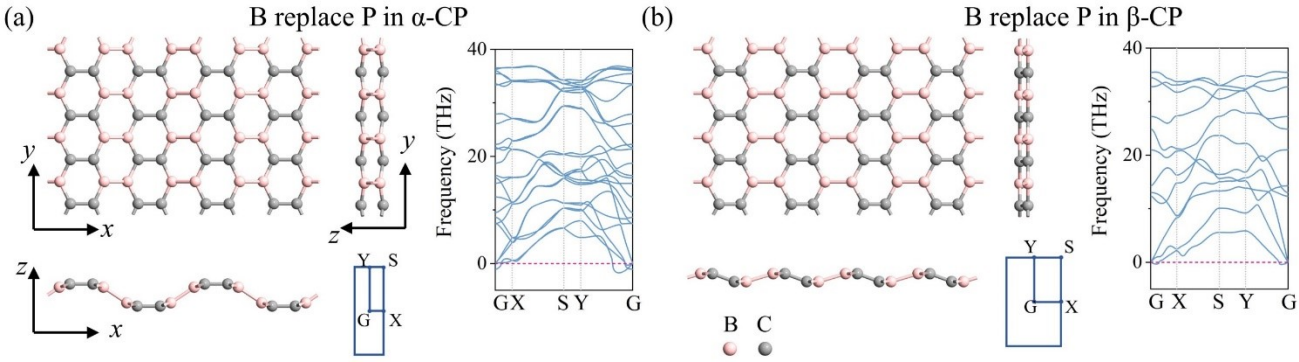

Fig. S9 The top view, side view, Brillouin zone, and the phonon dispersions of (a) the entire replacement system of the P-α-B and (b) P-β-B systems.

Table S1 The energy differences of 64-atoms C-substituted systems supercell with AFM1, AFM2, and AFM3 order, separately. ΔE_{AFMx} is the energy differences between AFMx and FM orders and $\Delta E_{AFMx} = E_{AFMx}-E_{FM}$, where E_{AFMx} and E_{FM} are the total energy with AFMx and FM order respectively (x=1, 2, 3). T_n is the Néel temperature and T_c is the Curie temperature.

C-substituted	**ΔE_{AFM1} (eV)**	**ΔE_{AFM2} (eV)**	**ΔE_{AFM3} (eV)**	**Magnetic ground state**	**T_n (K)**	**T_c (K)**

α-Mn	**-0.16**	-0.04	-0.15	AFM1	91.5	/
α-Fe	**-0.22**	-0.14	-0.11	AFM1	190.6	/
β-Ti	-0.0003	0	**-0.0009**	AFM3	21.8	/
β-Cr	-0.04	**-0.06**	0.05	AFM2	81.1	/
β-Mn	**-0.17**	-0.07	-0.15	AFM1	162.0	/
γ-V	0.02	0.04	0.03	FM	/	86.8
γ-Cr	0.05	0.03	**-0.01**	AFM3	377.2	/

Table S2 The energy differences of 64-atoms P-substituted systems supercell with AFM1, AFM2, and AFM3 order, separately.

P-substituted	**ΔE_{AFM1} (eV)**	**ΔE_{AFM2} (eV)**	**ΔE_{AFM3} (eV)**	**Magnetic ground state**	**T_n (K)**	**T_c (K)**
α-Mn	0.06	0.14	0.17	FM	/	303.4
α-Fe	0.13	0.18	0.33	FM	/	356.2
α-Co	0.45	0.02	0.48	FM	/	302.2
β-Cr	**-0.2**	0.01	-0.18	AFM1	170.8	/
β-Mn	0.15	0.14	0.23	FM	/	335.1
β-Co	0.45	0.04	0.44	FM	/	156.7
β-Ni	0.53	0.12	0.41	FM	/	42.6
β-Si	**-0.06**	-0.05	-0.01	AFM1	96.5	/
γ-Cr	0.04	**-0.02**	0.07	AFM2	164.8	/
γ-Co	0.13	0.13	**-0.01**	AFM3	16.1	/

Table S3 Geometric properties of graphene and other new two-element 2D layered materials.

□	a_1(Å)	a_2(Å)	$R_{C\text{-}C}$ (Å)	$R_{C\text{-}B}$ (Å)	$R_{B\text{-}B}$ (Å)	$R_{B\text{-}P}$ (Å)	$R_{P\text{-}P}$ (Å)
Graphene	2.47	2.47	1.43	/	/	/	/
α-Orthorhombic boron phosphide	5.58	3.23	/	/	1.66	1.85	2.12
β-Orthorhombic boron phosphide	5.59	6.43	/	/	1.67, 1.68	1.87	2.15, 2.18
Monoclinic carbon boron	5.47	4.34	1.40, 1.43	1.52, 1.57	1.53, 1.76, 1.79	/	/

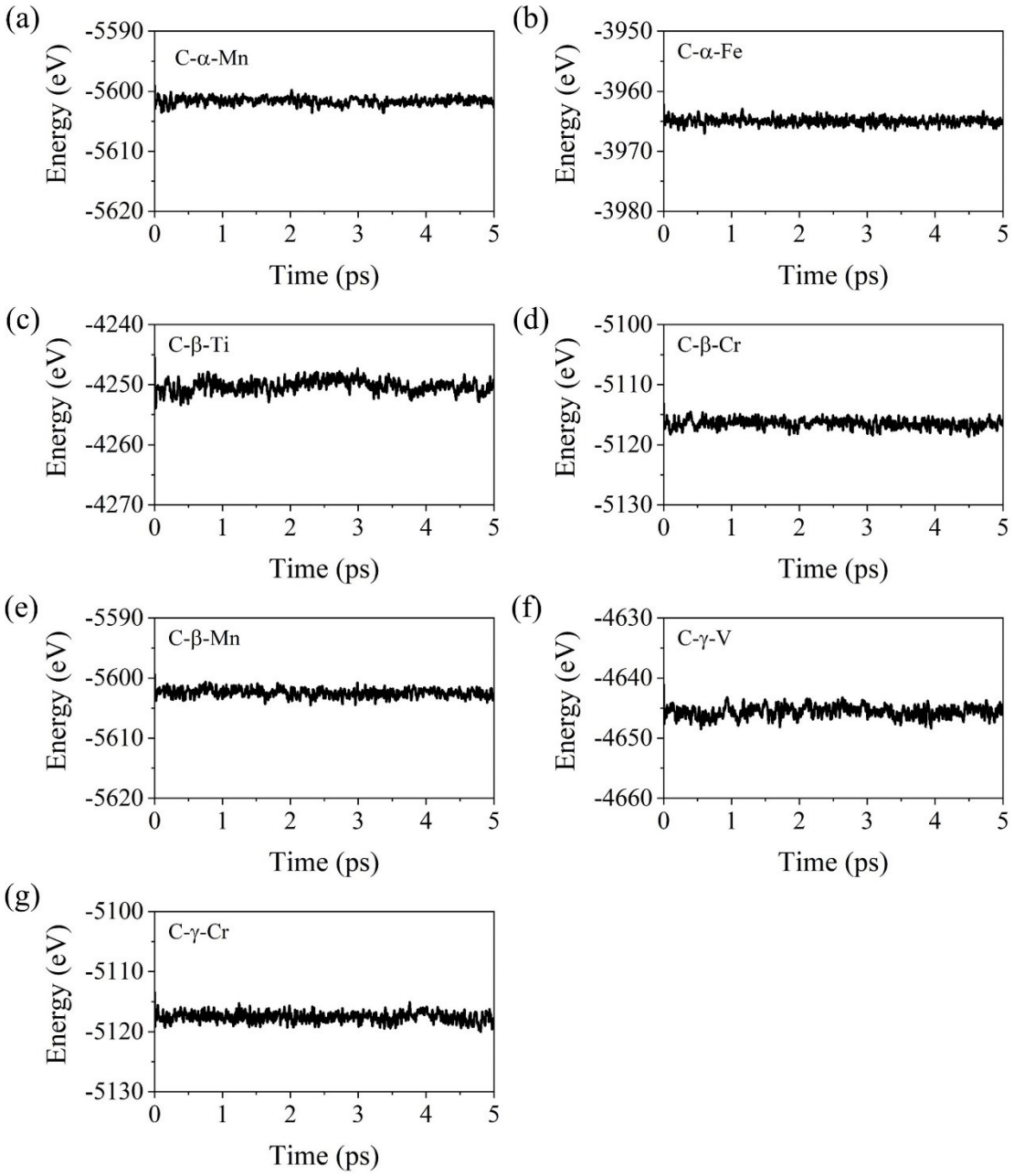

Fig. S10 The Ab initio molecular dynamics (AIMD) simulations for 7 half-metals based on C-substituted systems in 300K.

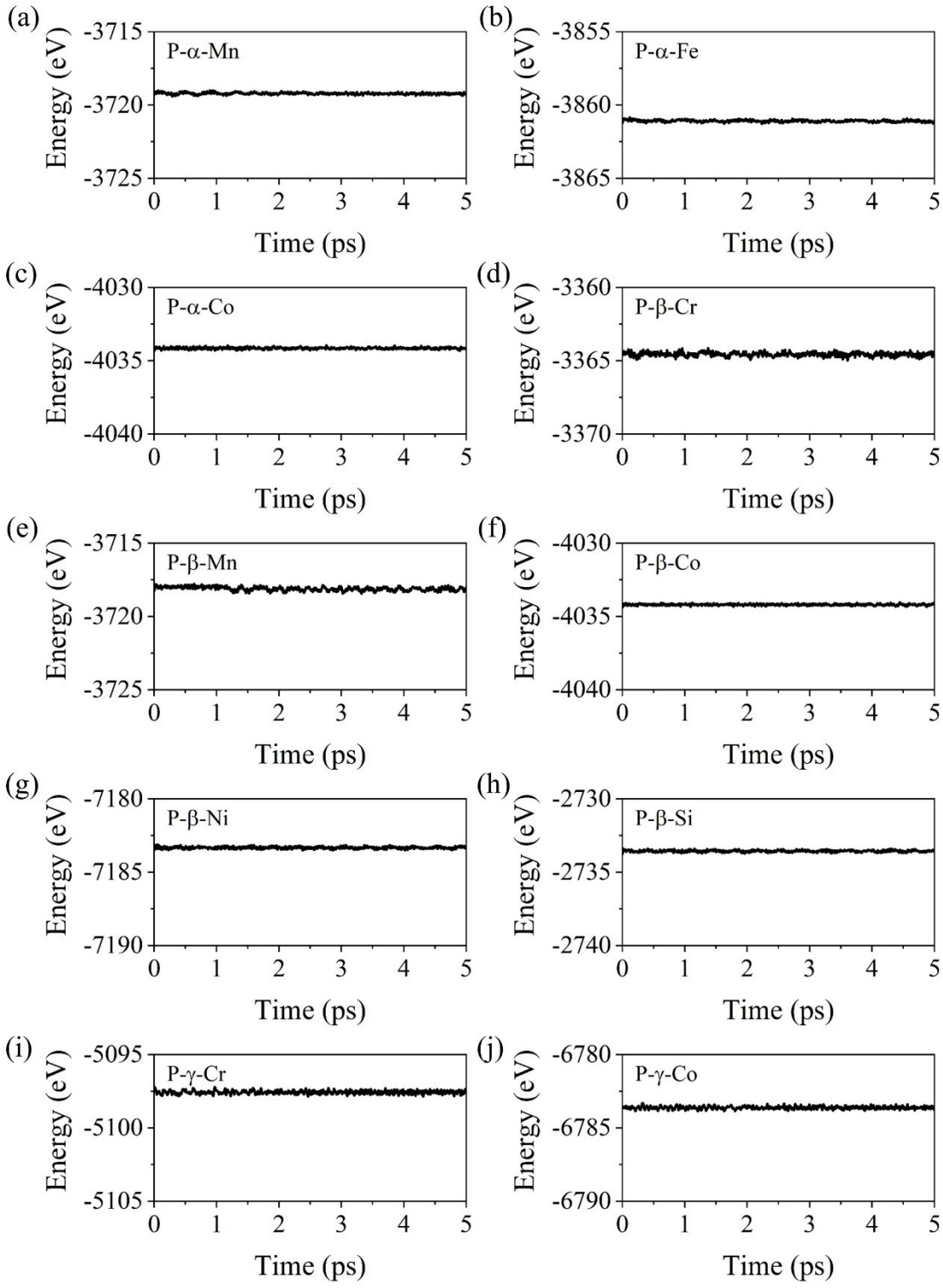

Fig. S11 The Ab initio molecular dynamics (AIMD) simulations for 10 half-metals based on P-substituted systems in 300K.

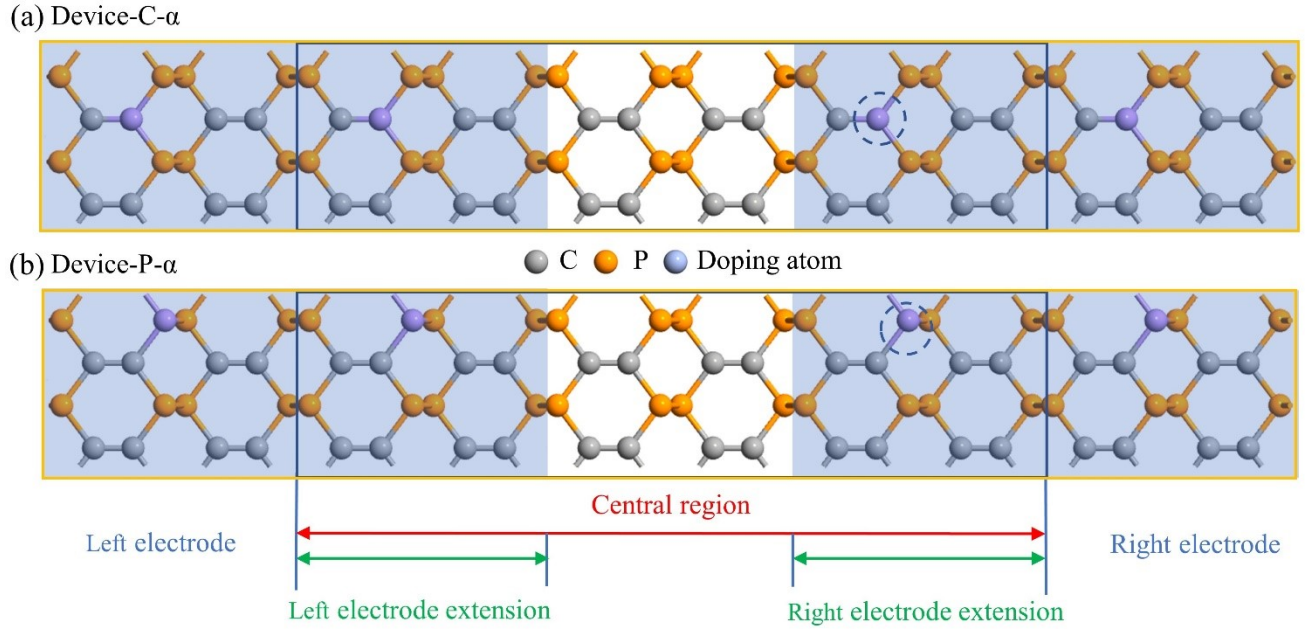

Fig. S12 The model of a half-metal device while the (a) C-atom substituted system based on α-CP or (b) P-atom substituted system based on α-CP as the electrode.

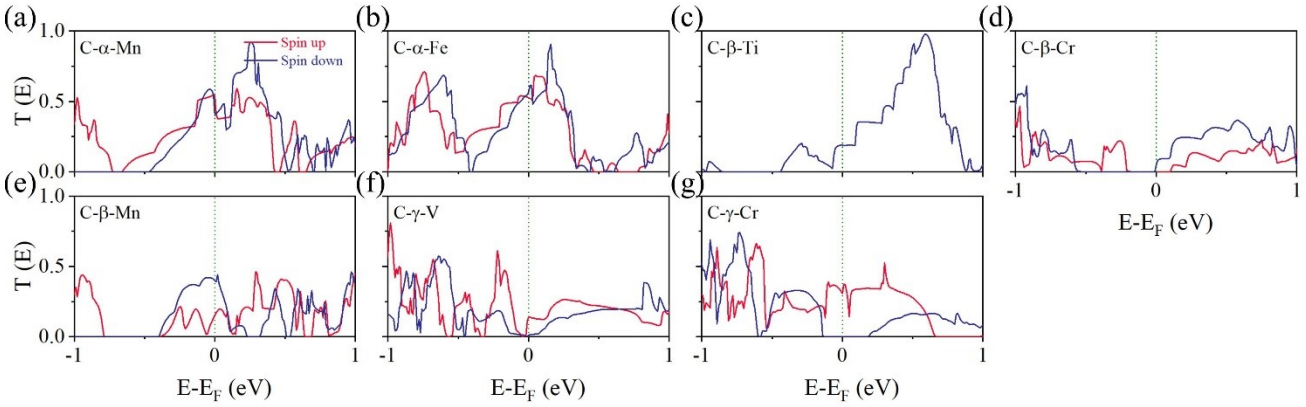

Fig. S13 The transmission spectra of 7 half-metal devices based on C-atom substituted systems in the PC setting under zero bias.

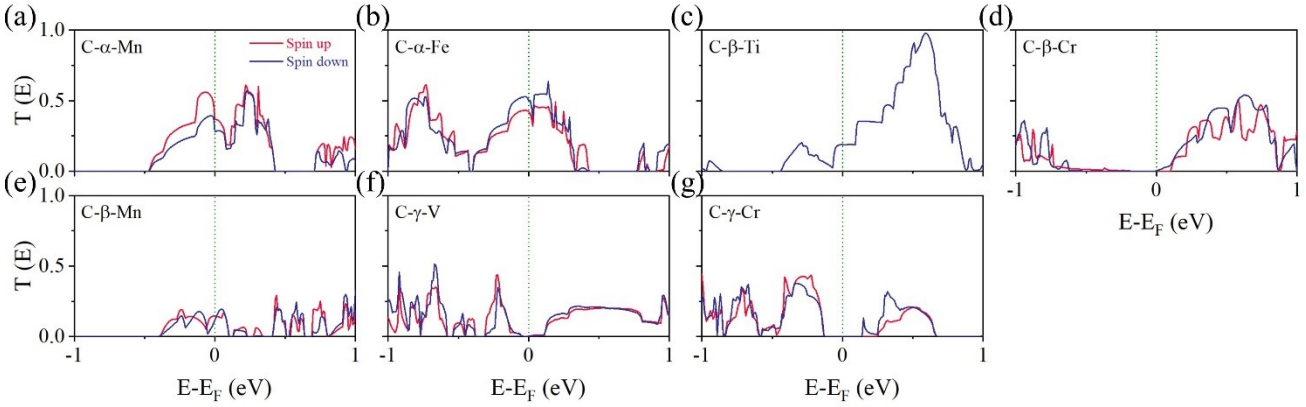

Fig. S14 The transmission spectra of 7 half-metal devices based on C-atom substituted systems in the APC setting under zero bias.

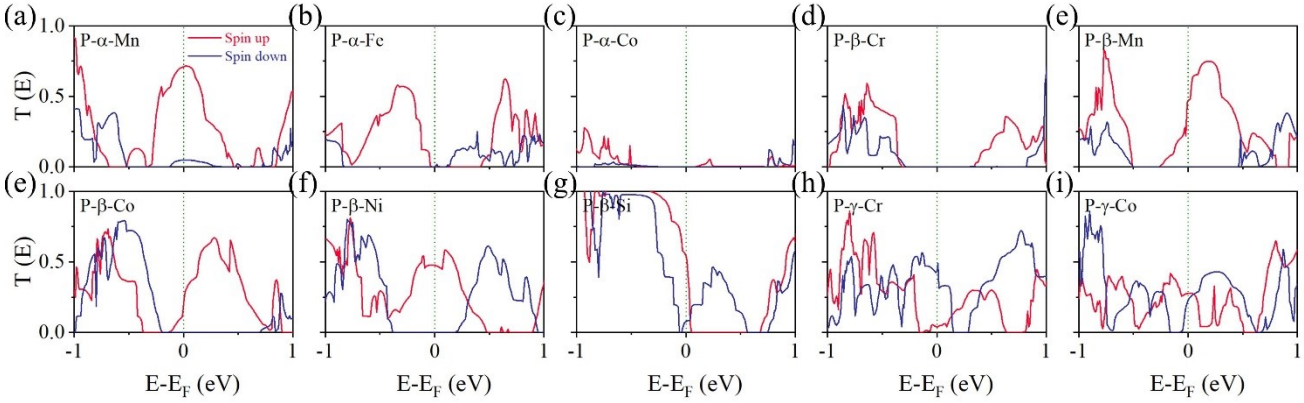

Fig. S15 The transmission spectra of 10 half-metal devices based on P-atom substituted systems in the PC setting under zero bias.

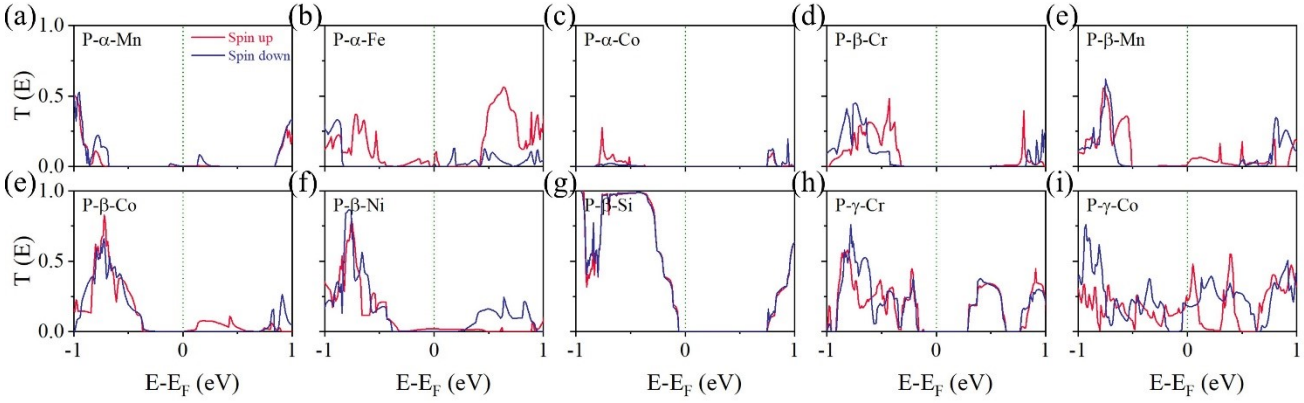

Fig. S16 The transmission spectra of 10 half-metal devices based on P-atom substituted systems in the APC setting under zero bias.

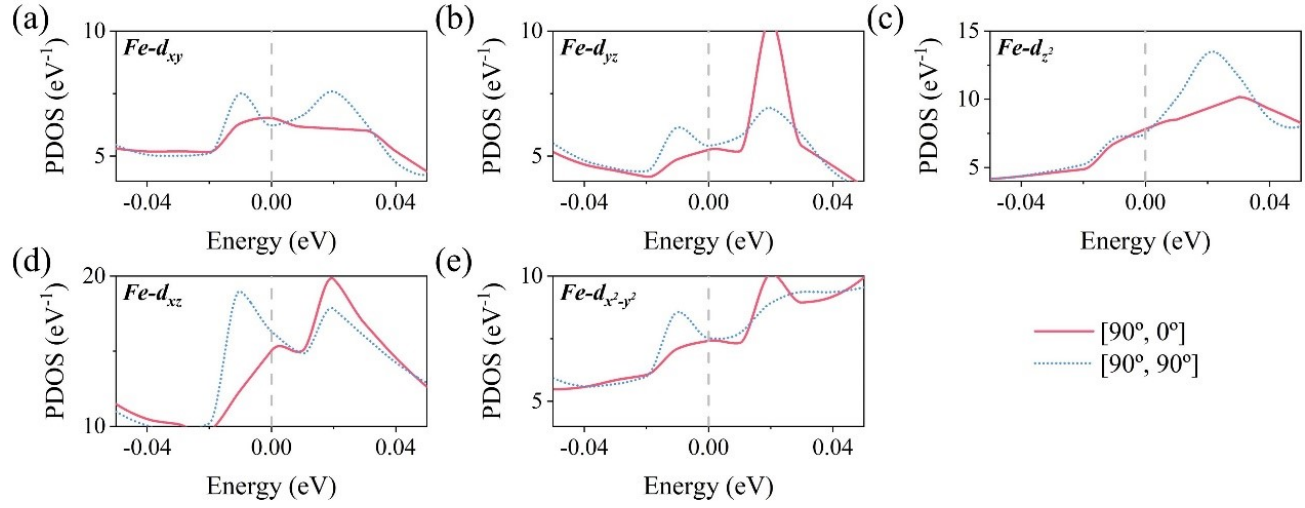

Fig. S17 The d orbital-resolved density of states for the Fe atom. The Fermi level is set to zero.

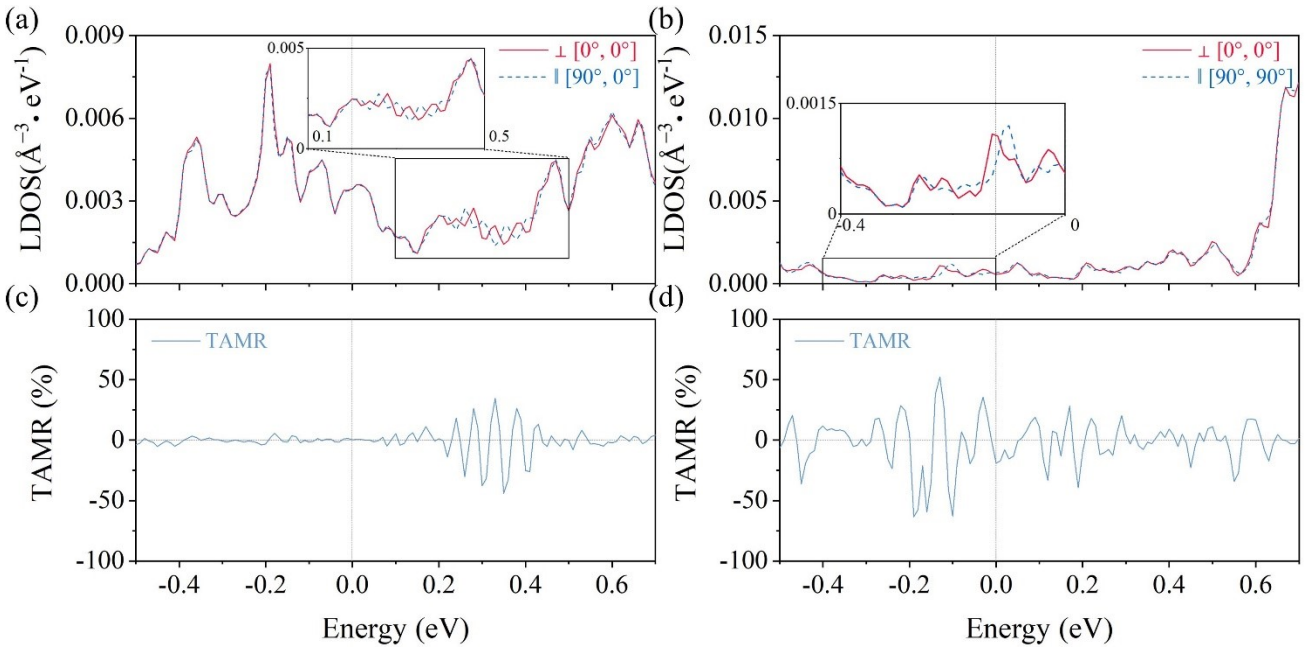

Fig. S18 The local density of states (LDOS) of the (a) C-α-Fe system and (b) P-β-Co system. The TAMR of the (C) C-α-Fe system and (d) P-β-Co system.